Paper No.
11232

NACE INTERNATIONAL CORROSION 2018 Conference & Expo

Mechanism of CO_2 Corrosion of Mild Steel: a New Narrative

Aria Kahyarian, Bruce Brown, and Srdjan Nesic
Ohio University
342 W. State St.
Athens, OH 45701
USA

ABSTRACT

The polarization behavior of API 5L X65 mild steel at various pH values and CO_2 partial pressures was investigated at a high flow velocity. In contrast to the commonly accepted mechanistic view of CO_2 corrosion, it is shown that the direct reduction of carbonic acid is insignificant at CO_2 partial pressures up to 5 bar. That suggests that carbonic acid is merely a "reservoir" of hydrogen ions and its presence only increases the observed limiting current densities by buffering the H^+ concentration at the metal surface. Furthermore, the rate of anodic iron dissolution reaction was shown to be significantly increasing in the presence of CO_2, suggesting that dissolved CO_2 or its associated carbonate species are directly involved in the iron dissolution reaction. The findings of the present mechanistic study showed that the increased corrosion rates of mild steel in acidic solutions in the presence of CO_2, which were previously associated with carbonic acid direct reduction, are in fact due to the increased rate of iron dissolution in the presence of CO_2, in combination with the increased cathodic limiting currents resulting from buffering ability of dissolved CO_2 and H_2CO_3.

Key words: Metallic corrosion, acidic corrosion, mild steel, carbon dioxide, mechanism, iron dissolution

INTRODUCTION

The profound effect of dissolved CO_2 on increasing the corrosion rate of pipeline steel, as compared to solutions of strong acids with the same acidity, has been known for many decades. However, findings in the last two decades have challenged the commonly accepted ideas about the underlying mechanisms of this process. This study is focused on the fundamentals of the electrochemical reactions involved in the CO_2 corrosion of mild steel in an attempt to further elucidate the mechanisms of the CO_2 corrosion process.

Carbon dioxide (CO_2) in gaseous or dissolved state is non-corrosive. However, upon dissolution in water (reaction (1)) and a subsequent hydration reaction (reaction (2)), a more reactive chemical species, carbonic acid (H_2CO_3), is formed. This hydration reaction is followed by dissociation reactions (reactions (3) and (4)) to form bicarbonate (HCO_3^-), carbonate (CO_3^{2-}), and hydrogen (H^+) ions; resulting in an acidic, corrosive solution.

$$CO_{2(g)} \leftrightharpoons CO_{2(aq)} \quad (1)$$

$$CO_{2(aq)} + H_2O_{(l)} \leftrightharpoons H_2CO_{3\,(aq)} \quad (2)$$

$$H_2CO_{3(aq)} \leftrightharpoons HCO_{3\,(aq)}^{-} + H^{+}{}_{(aq)} \quad (3)$$

$$HCO_{3\,(aq)}^{-} \leftrightharpoons CO_{3\,(aq)}^{2-} + H^{+}{}_{(aq)} \quad (4)$$

$$H_2O_{(l)} \leftrightharpoons OH^{-}{}_{(aq)} + H^{+}{}_{(aq)} \quad (5)$$

The chemical equilibria and water chemistry associated with dissolved CO_2 and its carbonate derivatives has been extensively studied. A more comprehensive discussion on this matter can be found elsewhere.[1,2]

Cathodic reactions in CO_2 Corrosion

The electrochemical reactions associated with CO_2 corrosion, based on the commonly accepted mechanisms, are shown below.[3–6] Anodic reaction (6) is the cause of metal deterioration, and reactions (7) through (10) are the commonly accepted cathodic reactions, providing the electron sink required for the anodic reaction to progress spontaneously. This mechanism is mainly based on the original studies of de Waard and Milliams in 1975, [7] Schmitt and Rothmann in 1977, [8] and Gray et al. in 1989 and 1990, [9,10] as reviewed in more details elsewhere. [1,2,6]

$$Fe^{2+}{}_{(aq)} + 2e^{-} \leftrightharpoons Fe_{(s)} \quad (6)$$

$$H^{+}{}_{(aq)} + e^{-} \leftrightharpoons \frac{1}{2}H_{2(g)} \quad (7)$$

$$H_2O_{\,(l)} + e^{-} \leftrightharpoons OH^{-}{}_{(aq)} + \frac{1}{2}\,H_{2(g)} \quad (8)$$

$$H_2CO_{3(aq)} + e^{-} \leftrightharpoons HCO_{3\,(aq)}^{-} + \frac{1}{2}\,H_{2(g)} \quad (9)$$

$$HCO_{3\,(aq)}^{-} + e^{-} \leftrightharpoons CO_{3\,(aq)}^{2-} + \frac{1}{2}\,H_{2(g)} \quad (10)$$

The effect of homogeneous chemical reactions of the water/CO_2 system on the rate of electrochemical reactions is probably the most important aspect of CO_2 corrosion that differentiates the uniform CO_2 corrosion from the corrosion induced by strong acids (e.g. HCl or H_2SO_4) or other weak acids such as H_2S and organic acids. There are two known effects associated with homogeneous chemical reactions in CO_2 corrosion:

a) The more significant effect is related to dissolved CO_2 gas. Only ~0.2 % of dissolved CO_2 molecules are hydrated to form H_2CO_3 according to the hydration equilibrium (reaction (2)). This means there is a large reservoir of dissolved CO_2 present in the solution to replenish the H_2CO_3 concentration as it is consumed by dissociation and/or reduction at the steel surface. Therefore, in addition to mass transfer of H_2CO_3 from the bulk solution, the limiting currents are increased as a result of this hydration reaction.
b) The second effect is associated with H_2CO_3 and its generic buffering ability as a weak acid. Considering the H_2CO_3 dissociation reaction (reaction (3)), the concentration of H^+ at the metal surface is buffered when the equilibrium shifts towards the right-hand side (i.e. consumption of H^+ by the reduction reaction). While this does not influence the magnitude of limiting current directly, it is of significance when discussing the mechanisms of charge transfer controlled corrosion at high CO_2 partial pressures.

The abovementioned mechanistic view of the cathodic reactions in CO_2 corrosion is now widely accepted, however, the new findings in more recent studies have challenged its foundations [11–13]. In those studies, it was shown quantitatively, that the limiting currents could be adequately explained even if H_2CO_3 was not considered an electroactive species. This can be understood when considering the local concentration of chemical species in the vicinity of the metal surface, where the homogeneous H_2CO_3 dissociation reaction (reaction (3)), followed by electrochemical reduction of the produced H^+ ions (reaction (7)), provides a parallel reaction pathway to the direct H_2CO_3 reduction reaction (reaction (9)). This observation carries a significant mechanistic implication, since it undermines the previous commonly accepted mechanistic arguments, which were developed based on the analysis of cathodic polarization behavior at or close to limiting currents [8–10]. Therefore, to date, the evidence for direct H_2CO_3 reduction is mostly circumstantial. This was perhaps best noted by Nordsveen et al. [11] who suggested that while the cathodic limiting currents can be quantitatively explained without considering H_2CO_3 as an electroactive species, the predicted corrosion rates are in better agreement with the experimental data when this additional reaction was included in the model.

The reaction mechanism that suggests H_2CO_3 dissociation is followed by H^+ reduction, is now known in the literature as the "buffering effect" mechanism, which was proposed as an alternative to the conventional mechanism including the carbonic acid reduction, the so called "direct reduction" mechanism. These proposed mechanisms are not particular to CO_2 corrosion. Similar arguments have been put forward for various weak acids such as acetic acid and hydrogen sulfide [14–17]. Considering a generic weak acid, HA, (representing: H_2CO_3, HCO_3^-, H_2S, HAc, etc.), its direct reduction can be expressed as reaction (11). As a weak acid that is only partially dissociated in the solution, HA is also involved in the homogeneous chemical equilibrium described *via* reaction (12). Additionally, in acidic solutions, the H^+ reduction reaction occurs as shown by reaction (13).

$$\mathrm{HA} + \mathrm{e}^- \longrightarrow \frac{1}{2}\mathrm{H}_2 + \mathrm{A}^- \qquad (11)$$

$$\mathrm{HA} \rightleftharpoons \mathrm{H}^+ + \mathrm{A}^- \qquad (12)$$

$$\mathrm{H}^+ + \mathrm{e}^- \longrightarrow \frac{1}{2}\mathrm{H}_2 \qquad (13)$$

The "direct reduction" mechanism suggests that HA reduction (reaction (11)) is significant, therefore, the cathodic currents in acidic solutions are the result of two parallel electrochemical reactions, HA reduction, and H^+ reduction. On the other hand, the "buffering effect" mechanism suggests that, reaction (11), the reduction of HA, is insignificant as compared to reaction (13), the reduction of H^+. Therefore, the dominant cathodic reaction in acidic solutions, is H^+ reduction, while HA buffers the concentration of H^+ ions at the surface through the homogeneous reaction (12). These two mechanisms may be qualitatively distinguished by studying the behavior of charge transfer controlled cathodic currents [14,15]. If the concentration of the common reactant between the two possible mechanisms (H^+) is kept constant, each mechanism shows a distinct behavior as the concentration of the weak acid is increased (Figure 1). For the case of the "buffering effect" mechanism, no significant change in charge transfer controlled currents is expected, since the weak acid is not electrochemically active (Figure 1.B). On the other hand, for the "direct reduction" mechanism the charge transfer controlled cathodic currents are increased as the concentration of the reactant (the weak acid) is increased (Figure 1.A). It is important to note that the magnitude of the limiting current in both mechanisms are identical and the shape of the limiting current does not provide conclusive evidence for the electrochemical activity of a chemical species.

Considering these two hypothetical behaviors, Tran et al. studied the effect of H_2CO_3 in CO_2 corrosion[18]. The authors noted that, even at higher CO_2 partial pressures the pure charge transfer control cathodic currents are not clearly observed on an X65 mild steel surface and this hypothetical behavior cannot be

verified. Therefore, stainless steel electrodes, being a more noble substrate, were used to eliminate the interference by the anodic iron dissolution reaction. By comparing the steady state voltammograms for pH 4 and pH 5 at 1 and 10 bar CO_2 partial pressures, the authors reported a behavior resembling that shown in Figure 1.B, and hence concluded that the cathodic currents in CO_2 saturated solutions follow the "buffering effect" mechanism[18]. However, considering the effect of alloying compounds of stainless steel (~ 20 wt. % Cr, and 10 wt. % Ni) and their corresponding passive films on the electro-activity of the metal surface, the observed mechanism for cathodic currents could not be applied to mild steel without further verification.

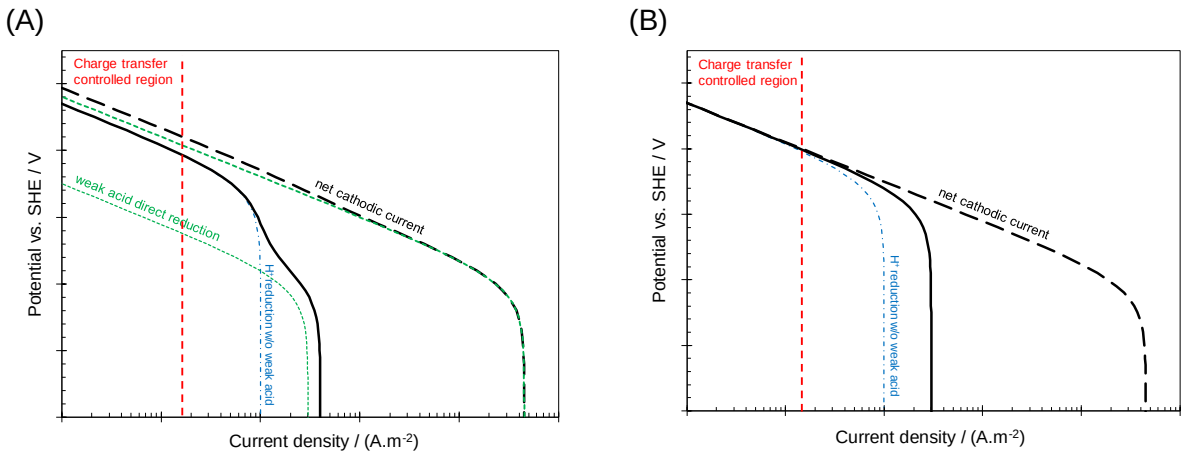

Figure 1: Hypothetical cathodic steady state voltammograms for (A) Direct reduction mechanism and (B) Buffering effect mechanism.

Anodic reactions in CO_2 corrosion

Iron oxidation as the dominant anodic reaction is a key element in acidic corrosion of mild steel. The mechanism of the iron oxidation reaction in acidic media has been extensively studied over the last few decades.[19–30] In this section, the mechanism of acidic iron dissolution is briefly discussed to provide the necessary context relevant to CO_2 corrosion, while a thorough review of the existing literature can be found elsewhere. [29,31]

El Miligy et al. [22] showed that the iron dissolution in mildly acidic environments occurs in four different states, depending on the potential and solution pH. The authors categorized these as *active dissolution*, *transition*, *pre-passivation*, and *passivation*, as demonstrated in Figure 2. Each range was shown to have a different electrochemical behavior, characterized by different apparent Tafel slopes and reaction orders. The peak potentials of the two local current maxima, observed in transition and pre-passivation ranges, were shown to be pH dependent. This suggests that the governing mechanism of iron dissolution at the corrosion potential could vary depending on the solution pH and other environmental conditions.

There are two classic mechanisms proposed for iron dissolution in acidic solutions in the literature, which are commonly referred to as: the "catalytic mechanism" and the "consecutive mechanism". These two mechanisms are associated with two distinct electrochemical behaviors observed in the active dissolution range. The catalytic mechanism, first proposed by Heusler et al. [32], is based on the experimental Tafel slope of 30 mV and second order dependence on hydroxide (OH^-) ion concentration. On the other hand, the consecutive mechanism proposed by Bockris et al. [27], was formulated to explain the observed Tafel slope of 40 mV and a first order dependence on OH^- ion concentration. These two significantly different

reaction kinetics are believed to be caused by the surface activity and microstructure of the metal substrate. [20,28,30,31] In more recent years there seems to be a consensus that these two mechanisms are in fact occurring in parallel. That can be seen in the so called "branching mechanism" proposed by Drazic, [28] which includes two parallel dissolution pathways: one resulting in a 40 mV Tafel slope and a first order pH dependence, and the other with a 30 mV Tafel slope and a second order pH dependence. The author suggested that the change of the mechanism between these two scenarios occurs with variation in the adsorption energy of the intermediate species that are affected by the steel microstructure or the environmental conditions. It was also suggested that the observed pH dependences ranging between 1 and 2 occurs when both mechanisms are at play simultaneously. A mechanism including parallel pathways was also proposed in the more comprehensive work of Keddam et al. [24,25] The authors proposed a mechanism including 7 elementary steps, resulting into 3 parallel dissolution pathways that incorporated the elementary steps for both the consecutive and the catalytic mechanisms.

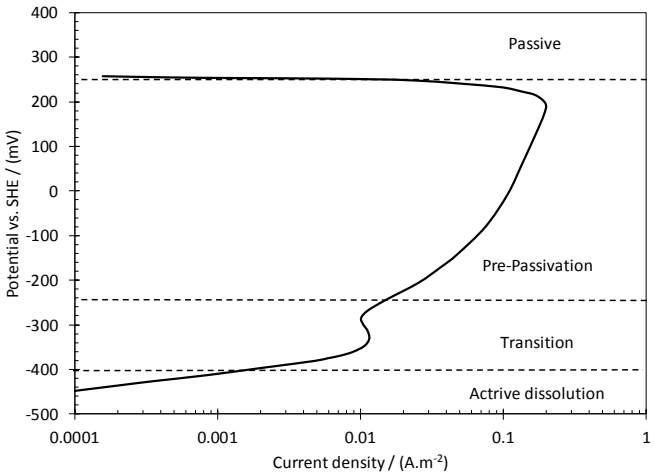

Figure 2: Anodic polarization curve of iron in 0.5 M Na_2SO_4 solution at pH 5 and 298˚K. With the scan rate of 6.6 mV.s^{-1} and rotating disk electrode at 69 rps. Data taken from El Miligy et al. [22]

The anodic polarization curves obtained for mild steel dissolution in acidic CO_2-saturated aqueous environments have frequently been reported to have a 40 mV Tafel slope and a first order dependence on hydroxide ion concentration. [9,10,33–35] The literature, as it relates to CO_2 corrosion, appears to be settled on the consecutive mechanism proposed by Bockris et al. [27] which has been frequently used to describe the anodic currents without considering any effect of dissolved CO_2 or the related carbonate species present in the solution. [9,33,36–39]

An in-depth analysis on the possible effect of dissolved CO_2 and/or other carbonate species on the iron oxidation reaction in acidic solutions is not available in the literature. Nevertheless, a significant effect of carbonate species on the rate of iron dissolution has been mentioned in a few different studies over the years [23,34,40–43]. The rate of anodic dissolution of iron in mildly alkaline solutions was shown to be increased in the presence of bicarbonate ions in several studies [41–43]. It that pH range, the anodic polarization curves showed that the iron dissolution reaction was at the passivation and trans-passivation range. There is a general agreement in the literature that the increasing rate of anodic dissolution is a result of chemical reaction of bicarbonate ion with the passive layer (e.g. $Fe(OH)_2$ and Fe_2O_3) to form various more soluble iron-complex species. [41–43]

The effect of CO_2 on the iron dissolution reaction was also studied by Linter and Burstein [40] at the pH range more relevant to the present study (pH 4). It was reported that the rate of iron dissolution from 0.5 Cr alloyed steel increased significantly in the transition and pre-passivation range, while the active dissolution range remained unaffected. Similar to what was proposed in previous works, [41–43] the authors associated this effect to destabilization of the passive layer through a chemical attack and complex formation by CO_2 or its related carbonate species [40]. In a study by Nesic et al. [23] the anodic polarization curves were used to discuss the effect of CO_2 in a relatively narrow potential range (~100 mV) above the corrosion potential. Experiments were performed in acidic perchlorate solutions (pH 2 to pH 6), and partial pressure of CO_2 limited to the 0 to 1 bar range. The proposed mechanism by Nesic et al. suggests that CO_2 is actively engaged in the electrochemistry of iron dissolution by directly adsorbing onto the metal surface and forming a chemical ligand that replaced the ferrous hydroxide intermediate species. The authors suggest that the presence of CO_2 did not affect the observed Tafel slopes, whereas the exchange current densities increased with a linear proportionality to pCO_2 up to 1 bar. Furthermore, it was noted that as $pCO_2 \rightarrow 1$ bar, the effect of CO_2 reaches its maximum and the rate of anodic reaction was not further increased with increasing pCO_2. In a more recent study, Almedia et al. [44] revisited this subject by investigating the corrosion of X65 mild steel at pCO_2=0, 1, and 30 bar. Based on electrochemical impedance measurements at corrosion potential, the authors concluded that CO_2 does not directly act on the metal surface and it has no significant effect on the iron dissolution reaction, in contrast to what was proposed by Nesic et al. [23] Nevertheless, considering that this mechanistic argument is developed merely based on measurements at the corrosion potential and only at pH 4, the reported mechanistic behavior may not be reasonably generalized to the wide range of conditions typically encountered in CO_2 corrosion.

Despite the reported influence of CO_2 on the iron dissolution reaction, the current narrative of the CO_2 corrosion mechanism in the literature does not account for this mechanistic aspect. The present study is an attempt to further elucidate the possible influence of CO_2 or its related carbonate species on the rate of steel dissolution in mildly acidic environments relevant to CO_2 corrosion. The investigation of the anodic behavior in the presence of CO_2 complements the findings in the first part of this study on the cathodic reactions, in order to provide a more inclusive description of the effect of CO_2 on acidic corrosion of mild steel.

EXPERIMENTAL PROCEDURE

The experiments were conducted in a thin channel flow cell (TCFC) described in detail elsewhere [45–49]. The test section was modified for electrochemical measurements by introducing a saturated Ag/AgCl reference electrode facing the working electrode (3.175 mm apart), as shown in Figure 3. The TCFC stainless steel structure was used as the counter electrode.

A 0.1 M NaCl supporting electrolyte solution (110 L), used throughout this study, was initially purged for ~ 3 hr, with N_2 or CO_2 gas depending on the experimental conditions, while the outlet gas was monitored with an oxygen sensor (Orbisphere 410). Maximum dissolved oxygen content before initiating the experiment was 3 ppb (typically ~1 ppb). For experiments at elevated pCO_2, this deoxygenation step was followed by pressurizing the system to 5 bar for at least 3 hr, or until a steady pH was obtained. As the last step, the pH was adjusted to the target value by gradual addition of deoxygenated HCl or NaOH solutions into the system. The temperature was controlled (±0.5°C) by means of electric heaters placed in the tank and in the test section (used for experiments at 30°C) as well as a heat exchanger (used for experiments at 10°C) connected to a chiller (Air-3000 FLUID CHILLERS Inc.). The pump output was fixed throughout the experiments such that the flow velocity of 11 $m.s^{-1}$ was obtained inside the thin channel test section (3.3E-4 m^2 cross sectional area).

The disk shaped working electrodes were made of API 5L X65 mild steel with the same chemical composition as reported in our earlier study.[14] Prior to each experiment, the electrodes were abraded with a 600 grit silicon carbide paper and rinsed and sonicated in isopropanol for 5 minutes. After inserting the working electrodes into the test section, the test section was purged using dry N_2 or CO_2 gas. After introducing the solution into the test section, the measurements were carried out following a 15 min rest at open circuit potential (OCP) in order to assure a stable readout. The polarization curves reported in the present study were obtained using staircase voltammetry at 0.5 $mV.s^{-1}$ scan rate and 1 s^{-1} sampling period. The anodic and cathodic polarizations were obtained in separate experiments by sweeping the potential from OCP towards more positive and more negative potentials, respectively. The reported polarization curves were corrected for ohmic drop with the solution resistance obtained by electrochemical impedance spectroscopy (EIS) measurements (DC potential 0 mV vs. OCP, AC potential 5 mV, frequency range 100KHz to 0.2 Hz at 10 points/dec), after polarization measurements and a 15 min rest so that a stable OCP was reached. The LPR measurements were also carried out in separate experiments, following the above mentioned preparation sequence, using a ±5 mV potential range and the scan rate of 0.125 $mV.s^{-1}$.

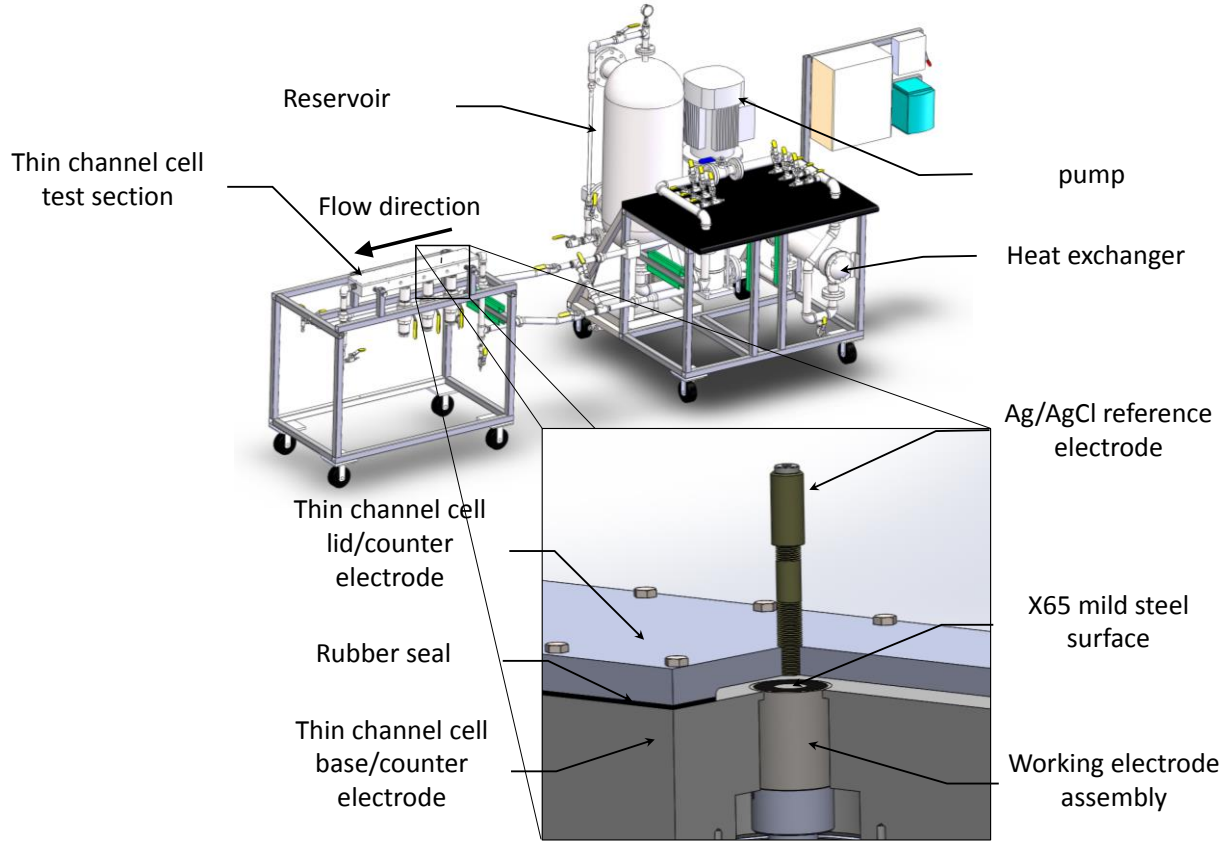

Figure 3. The experimental setup and electrode arrangement inside the thin channel flow test section.

RESULTS AND DISCUSSION

The experimental conditions were designed to improve the likelihood of observing the charge transfer controlled cathodic currents, needed to verify one of the hypothetical behaviors shown in Figure 1. The polarization curves obtained on API 5L X65 mild steel surface at pH 4 and pH 5 are shown in Figure 4.A and Figure 4.B, respectively. These experimental results revealed a notable influence of CO_2 on both cathodic and anodic polarization curves.

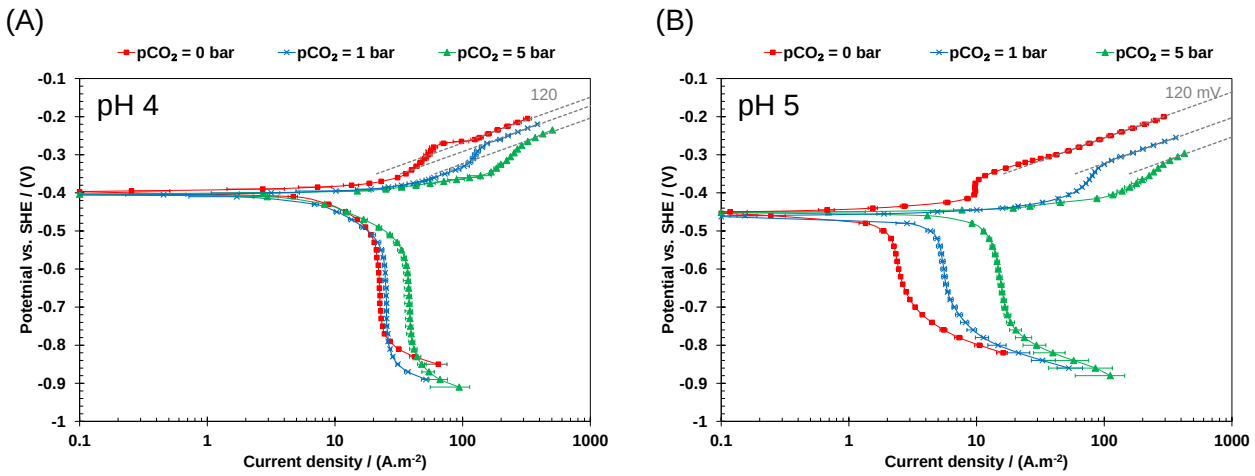

Figure 4. Polarization curves at 30ºC, 11 m.s^{-1}, 0.1 M NaCl, 0.5 mV.s^{-1} scan rate on an X65 mild steel surface. A) pH 4, B) pH 5.

The effect of pCO_2 on the cathodic limiting current density is now well understood. A detailed evaluation of this parameter requires comprehensive calculations that accounts for the mass transfer of numerous species and their interaction through homogenous chemical reactions inside the boundary layer.[1,2] However, an estimate can be obtained considering that the magnitude of the limiting current density in CO_2 saturated solutions is the same whether carbonic acid was assumed to be electroactive or not.[11,13] That suggests the kinetics of the carbonic acid dissociation reaction are fast enough so that the concentrations of involved species reaches a quasi-equilibrium state. The reported experimental data in the present study show that carbonic acid is not electrochemically active, as discussed further in the following paragraphs. However, at mass transfer limiting conditions the surface concentration of carbonic acid can be assumed to be close to zero since the local concentration of H^+ is close to zero and that is directly reflected on the concentration of carbonic acid through the homogenous dissociation reaction. Therefore, while H_2CO_3 is not reduced directly, its flux can be calculated in the same fashion to that of an electrochemically active species. Knowing that all the H_2CO_3 transferred to the surface is eventually consumed through the H^+ reduction reaction, the limiting current density can be expressed as the superposition of the limiting current arising from the mass transfer of H^+ and that of H_2CO_3.

The limiting current density can be obtained if the mass transfer coefficient is known. The mass transfer coefficient (k_m) for a thin channel flow can be obtained via the same correlations proposed for pipe flow, using the equivalent hydraulic length:[50]

$$\frac{k_m l_{eq}}{D} = Sh = 0.0165\, Re^{0.86} Sc^{0.33} \qquad (14)$$

where D is the diffusion coefficient ($m^2.s^{-1}$), Sh is the Sherwood number, Re is the Reynolds number, Sc is the Schmitt number, and l_{eq} is the equivalent hydraulic length (m). The equivalent hydraulic length for a thin channel flow was calculated using $4A/P$=*7.1 mm*, where $A\ (m^2)$ is the flow cross section area and $P\ (m)$ is the wetted wall perimeter. The limiting current density of H^+ was calculated using Equation (15), where F (Col.eq^{-1}) is the Faraday's constant, and C_{H+} (mol.m^{-3}) is the concentration of hydrogen ion:

$$i_{lim,H^+} = F k_m C_{\mathrm{H}^+} \qquad (15)$$

The limiting current arising from H_2CO_3 was calculated *via* Equations (16) and (17) as discussed by Nesic et al. [51], in order to account for the effect of CO_2 hydration reaction.

$$i_{lim,H_2CO_3} = F\, C_{\mathrm{H_2CO_3}} \sqrt{k_{hyd,b} D}\, \coth \xi \qquad (16)$$

$$\xi = \frac{D/k_m}{\sqrt{D/k_{hyd,b}}} \qquad (17)$$

where k_m is the mass transfer coefficient from Equation (14), $k_{hyd,b}$ is the rate constant of CO_2 dehydration reaction [52], ξ is the ratio of the "mass transfer layer thickness" over the "chemical reaction layer thickness", and $C_{\mathrm{H_2CO_3}}$ (mol.m^{-3}) is the equilibrium concentration of carbonic acid that can be obtained as discussed elsewhere [2,11]. The total limiting current densities ($i_{lim,H^+} + i_{lim,H_2CO_3}$), calculated as described above, were compared with those obtained experimentally as shown in Figure 5.

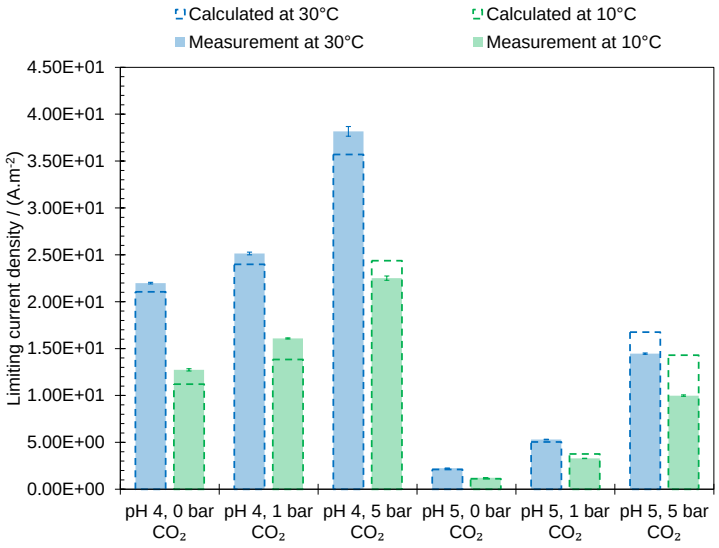

Figure 5 . The comparison of the experimental limiting current densities shown in Figure 4 (solid bars) with the calculated values (dashed bars). The error bars represent the standard deviation of three measurements.

In Figure 4, the charge transfer controlled cathodic currents were to some extent observed at pH 4, which were not significantly increased as the pCO_2 was increased. Considering the aforementioned hypothetical behavior (Figure 1.B), these results suggest that carbonic acid was not significantly reduced during the cathodic polarization measurements. However, at pH 5 the cathodic currents were under mass transfer/chemical reaction control at all pCO_2 values, hence, the hypothesis could not be properly verified.

Over the anodic current range, the polarization curves showed a significant effect of pCO_2 on the electrochemical behavior of the iron dissolution reaction. Considering the categorization of El Miligy et al., [22] the results reported in Figure 4 only show the transition and the pre-passivation ranges, while the active dissolution range was covered by the cathodic currents. As shown by the guidelines in Figure 4, the pre-passivation range was found to be reasonably quantified with a 120 mV Tafel slope. The guidelines were used to obtain the reaction order versus pH and pCO_2. Comparing the anodic curves where no CO_2 was present showed a negligible dependence on the solution pH, which was found to agree with that previously reported in the literature. [22,53,54] In the presence of CO_2, while the Tafel slope in the pre-passivation range was not affected, reaction orders of 0.34 and 0.61 vs. pCO_2 were observed at pH 4 and pH 5, respectively.

In order to improve the likelihood of observing the effect of CO_2 on the charge transfer cathodic currents and the anodic currents at the active dissolution range, a set of experiments at a lower temperature (10°C) were conducted in the present study. Decreasing the temperature was expected to influence the observed polarization curves though number of different processes:

a) The mass transfer coefficient and the rate of hydration reaction would decrease by decreasing the temperature (decreasing the limiting current), while the solubility of CO_2 in water increases (increasing the limiting current).
b) The charge transfer controlled currents would decrease exponentially, following the Arrhenius law.

Overall, one could expect that the charge transfer controlled currents to decrease with decreasing temperature more effectively than the limiting currents would, which broadens the potential range where one can observe the charge transfer controlled currents. Additionally, decreasing the rate of both anodic and cathodic reactions at a low current density range would reveal more details of the kinetics of iron dissolution in the active dissolution range.

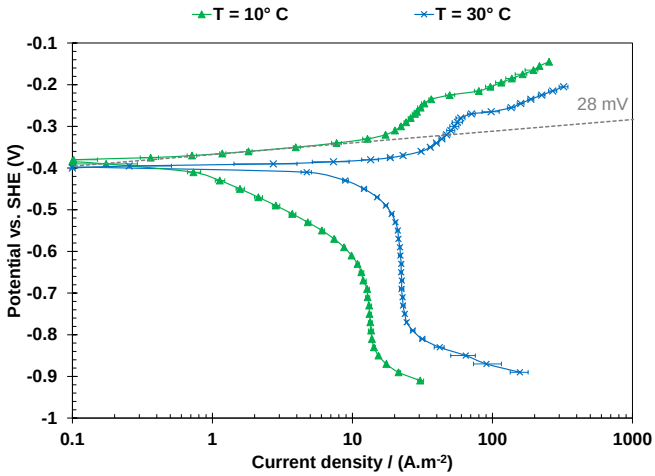

Figure 6. Temperature dependence of polarization curves at pH 4, pCO_2=0 bar, 11 $m.s^{-1}$, 0.1 M NaCl, 0.5 $mV.s^{-1}$ scan rate on X65 mild steel surface.

The effect of temperature on polarization curves obtained on X65 mild steel at 10°C and 30°C is shown in Figure 6. The results at 10°C showed a clear Tafel behavior for the cathodic currents, indicating a charge transfer controlled range. Additionally, a linear range in anodic currents with the Tafel slope of ~28 mV was observed, which is associated with the active dissolution range for the anodic reaction. The

clear separation between the cathodic and anodic currents observed at lower temperature provides a great opportunity for better understanding the effect of CO_2 on the electrochemical behavior of iron in acidic solutions.

The polarization curves obtained at 10°C, various pCO_2, and at pH 4 and 5 are shown in Figure 7.A and B, respectively. Over the cathodic current range, at pH 4, the charge transfer controlled current (Tafel) range were clearly observed at all pCO_2 values up to 5 bar, and were not significantly affected by the presence of CO_2. This behavior was similar to that observed at 30°C (Figure 4.A) and the hypothetical behavior shown in Figure 1.B that further supports the argument that carbonic acid was not reduced on the X65 mild steel surface during cathodic polarization. At pH 5 and pCO_2=0 bar, the cathodic currents were still under mass transfer control at 10°C, however, the charge transfer controlled currents were observed at pCO_2=1 bar and pCO_2=5 bar. Here also the results suggest that increasing CO_2 partial pressure does not significantly increase the charge transfer controlled cathodic currents and that the so called "buffering effect" is the governing mechanism for carbonic acid contribution to the cathodic currents.

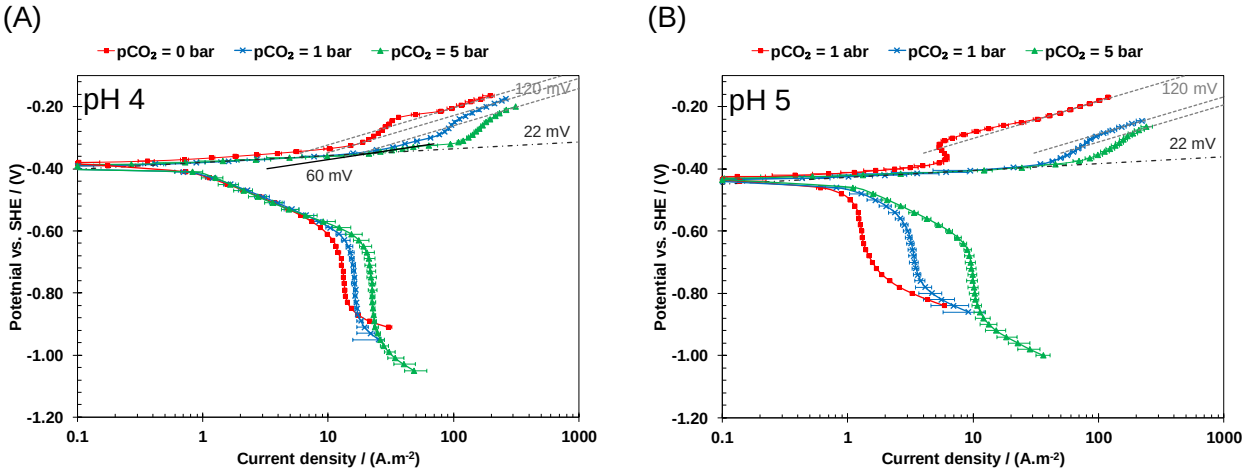

Figure 7. Polarization curves at 10°C, 11 $m.s^{-1}$, 0.1 M NaCl, 0.5 $mV.s^{-1}$ scan rate on an X65 mild steel surface. A) pH 4, B) pH 5.

Over the anodic current range, the polarization curves obtained at 10°C also showed the significant influence of CO_2 or, what is more likely, its associated carbonate species, on the kinetics and the mechanism of iron dissolution reaction. Figure 8 demonstrates the effect of pH on the observed anodic polarization curves obtained at 10°C and 30°C. At 30°C, only the transition and the pre-passivation ranges were observed, while the anodic polarization curves obtained at 10°C clearly demonstrate a range of anodic currents associated with the active dissolution range, in addition to the transition and pre-passivation range. The electrochemical behavior at the pre-passivation range is similar to that observed at 30°C. At the active dissolution range, a ~28 mV Tafel slope and a ~ -1.5 reaction order vs. H^+ concentration was observed.

The effect of pCO_2 on the iron dissolution reaction at pH 4 and pH 5 are shown in the polarization curves reported in Figure 7.A and Figure 7.B, respectively. In these graphs the active dissolution, transition and the pre-passivation ranges were observed clearly, while pCO_2 was shown to have a profound effect over the whole range. In the presence of CO_2, the Tafel slope in the active dissolution range slightly decreased from ~28 mV (in Figure 8) to ~22 mV (in Figure 7). The decrease in the Tafel slope in this range remained the same at higher CO_2 partial pressures. Furthermore, in the transition range, an additional linear

behavior with Tafel slope of ~60 mV was observed (most clearly at pH 4 and 5 bar CO_2). The pre-passivation range was also significantly affected by the pCO_2. In that range, the Tafel slope was ~120 mV for all pCO_2 values, similar to what observed at 30°C. The reaction orders vs. pCO_2 of 0.39 and 0.30 were observed for pH 4 and pH 5, respectively, which were somewhat lower than that observed at 30°C.

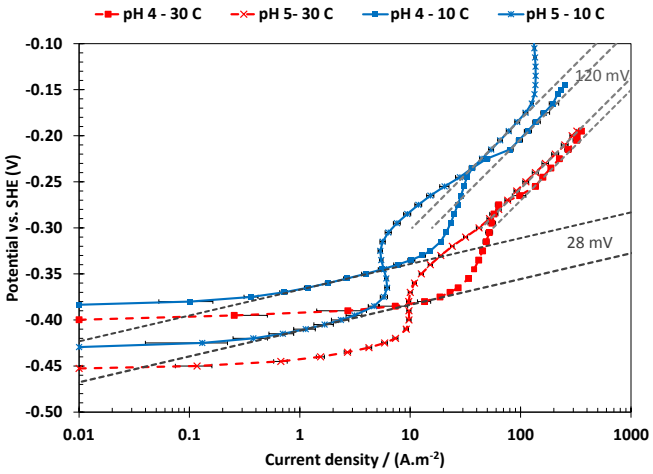

Figure 8. Anodic polarization curves at 11 $m.s^{-1}$ flow rate, 0.1 M NaCl, 0.5 $mV.s^{-1}$ scan rate on an X65 mild steel surface. Error bars represent the minimum and maximum values obtained in at least three repeats.

The observed influence of CO_2 on anodic reaction in active dissolution range was found to partially agree with the results reported by Nesic et al. [23] in the sense that the presence of CO_2 resulted in an increased rate of reaction which was not further intensified at pCO_2>1. However, in the present study the effect was in the form of a slight change of Tafel slope. Despite the fact that this effect was quantitatively small (only ~6 mV), it could still imply a change of mechanism. The 28 mV Tafel slope which correlates well with 1/2×2.303RT/F, is a characteristic of an electrochemical reaction preceded by one or more elementary steps, whereas the 22 mV Tafel slope (2/5× 2.303RT/F) may suggest an electrochemical reaction preceded by two or more elementary steps.

The significant increase of the anodic reaction rate in the transition and pre-passivation ranges appears to be in agreement with the results reported previously by Linter and Burstein.[40] In that study, the authors suggested that the increased rate of iron dissolution was a result of the destabilization of the passive layer, $Fe(OH)_2$ or Fe_2O_3 species, through a chemical attack by bicarbonate ion, similar to that proposed for the alkaline pH range.[41–43] Such an explanation may not be assumed to be valid for the conditions of the present study, considering that the formation of a passive layer on a mild steel surface is not thermodynamically favored at the pH and potential range of interest. [55] However, a rather similar chemical interaction of CO_2 or other associated carbonate species could be feasible for the conditions in the present study. The previously proposed mechanism of iron dissolution in acidic solutions without CO_2 suggests that the first current maximum observed in the polarization curves is associated with accumulation of the reaction intermediate Fe(I), i.e. FeOH, on the metal surface. [24,25,31] Keddam et al. suggest that the increased current after the first arrest is a result of a parallel reaction pathway involving Fe(II) intermediate species. [24,25,31] The second current maximum at more positive potentials leading to the surface passivation (not observed in the polarization curves presented here), was associated with a chemical transformation of Fe(II) intermediates into insoluble passivating species, e.g. $Fe(OH)_2$. [31] Therefore, the increase of current at the first peak could possibly be explained by an interaction of dissolved carbonate species with Fe(I) reaction intermediate, providing an additional chemical desorption

pathway for this species that could increase the observed current densities at the first peak. However, the observation of an additional 60 mV Tafel slope range below the first peak and the continuous increase of the exchange current density at the 120 mV range could also be a strong indication of electrochemical reactions where carbonate intermediate species are involved.

Developing a detailed mechanism for the iron dissolution reaction at these conditions requires a comprehensive investigation on the subject, considering the complexity of the reaction. However, the results presented here demonstrate a significant effect of CO_2 on the rate and the mechanism of iron dissolution in acidic environments. The more strongly influenced transition and pre-passivation ranges are of particular interest in the typical CO_2 corrosion scenarios. As shown in Figure 4, at pH values of 5 and higher, even at 30°C, the corrosion current is in the transition/pre-passivation range. The polarization curves clearly indicate that the effect of CO_2 on the anodic reaction rate is as significant as its effect on the cathodic limiting current density.

Effect of pCO_2 on corrosion rate

The effect of pCO_2 on corrosion rate of X65 mild steel was further discussed based on the experimental data obtained by LPR measurements. The change in corrosion rates with respect to CO_2 partial pressure at pH 4 and pH 5 are shown in Figure 9.A and B, respectively. The observed behavior was found to agree well with the abovementioned mechanistic discussion. At pH 4, increasing pCO_2 from 0 to 5 bar only resulted in a minor increase in the corrosion rates. In these conditions, the cathodic currents were under charge transfer control. Considering that carbonic acid was not directly reduced, increasing pCO_2 was not expected to result in any higher cathodic current. The minor increase of corrosion rates are associated with the slight increase of the anodic reaction rate in the active dissolution range by introducing CO_2.

The corrosion rates obtained at pH 5 demonstrate a rather different trend. At 10°C, as shown in Figure 9.B the cathodic currents were under charge transfer control, and anodic currents were in the active dissolution range. Hence, increasing pCO_2 did not result in significantly higher corrosion rates, similar to that observed at pH 4. On the other hand, at 30°C, the cathodic currents were under mass transfer control and the anodic currents were in the transition range, therefore, increasing pCO_2 significantly increased the observed corrosion rates from 2.8 $mm.y^{-1}$ at pCO_2=0 bar to 13.2 $mm.yr^{-1}$ at pCO_2=5 bar, by increasing both the mass transfer limiting current and the rate of anodic reaction in transition state.

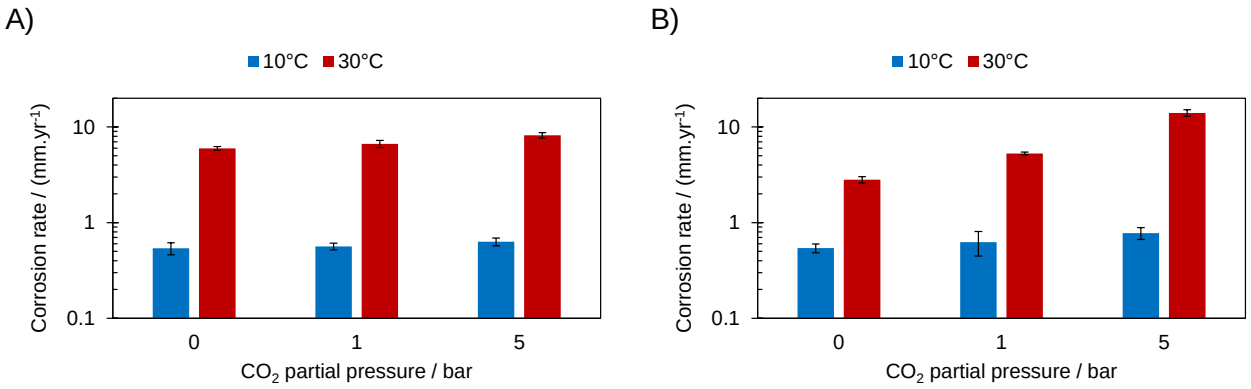

Figure 9: Corrosion rates obtained at 11 $m.s^{-1}$ flow rate and 0.1 M NaCl on X65 mild steel surface at 10°C and 30°C: A) pH 4, B) pH 5.

CONCLUSIONS

The polarization behavior of API 5L X65 mild steel at various pH and pCO_2 values was investigated at a high flow velocity and temperatures 30°C and 10°C. The electrochemical behavior of the cathodic and anodic reactions suggested that:

1- The direct reduction of carbonic acid was negligible. Therefore, the effect of CO_2 on the cathodic currents is primarily reflected on the limiting current, which increases due to: CO_2 hydration reaction that replenishes the surface concentration of carbonic acid and carbonic acid dissociation that buffers the H^+ concentration at the metal surface.

2- The rate of iron dissolution reaction was significantly increased in the presence of CO_2, suggesting that the mechanistic description previously developed in acidic aqueous solutions is not valid when CO_2 is present. The profound effect of CO_2 on anodic currents suggests that CO_2 or its related carbonate species are directly involved in the iron dissolution reaction.

3- Considering the abovementioned findings, the increased corrosion rates of mild steel in acidic solutions in the presence of CO_2 are due to the increased rate of iron dissolution in presence of CO_2, in addition to the increased cathodic limiting currents resulting from the buffering ability of dissolved CO_2 and H_2CO_3.

ACKNOWLEDGEMENTS

The author would like to thank the following companies for their financial support:
Anadarko, Baker Hughes, BP, Chevron, CNOOC, ConocoPhillips, DNV GL, ExxonMobil, M-I SWACO (Schlumberger), Multi-Chem (Halliburton), Occidental Oil Company, Petrobras, PTT, Saudi Aramco, Shell Global Solutions, SINOPEC (China Petroleum), TransCanada, TOTAL, and Wood Group Kenny.

REFERENCES

1. Kahyarian, A., M. Singer, and S. Nesic, *J. Nat. Gas Sci. Eng.* 29 (2016): pp. 530–549, http://dx.doi.org/10.1016/j.jngse.2015.12.052.
2. Kahyarian, A., M. Achour, and S. Nesic, "Mathematical Modeling of Uniform CO_2 Corrosion," in Trends Oil Gas Corros. Res. Technol., ed. A.M. El-Sherik (Elsevier, 2017), pp. 805–849.
3. Nešić, S., "Carbon Dioxide Corrosion of Mild Steel," in Uhlig's Corros. Handb. Third Ed. (2011), pp. 229–245.
4. Nešić, S., *Corros. Sci.* 49 (2007): pp. 4308–4338.
5. Kermani, M.B., and A. Morshed, *Corrosion* 59 (2003): pp. 659–683.
6. Kahyarian, A., M. Achour, and S. Nesic, "CO_2 Corrosion of Mild Steel," in Trends Oil Gas Corros. Res. Technol., ed. A. M. El-Sherik (Elsevier, 2017), pp. 149–190.
7. de Waard, C., and D.E. Milliams, *Corrosion* 31 (1975): pp. 177–181.
8. Schmitt, G., and B. Rothmann, *Werkstoffe Und Korrosion* 28 (1977): p. 816.
9. Gray, L.G.S., B.G. Anderson, M.J. Danysh, and P.R. Tremaine, "Mechanisms of Carbon Steel Corrosion in Brines Containing Dissolved Carbon Dioxide At pH 4," in CORROSION (1989), Paper No. 464.
10. Gray, L.G.S., B.G. Anderson, M.J. Danysh, and P.R. Tremaine, "Effect of pH and Temperature on the Mechanism of Carbon Steel Corrosion by Aqueous Carbon Dioxide," in CORROSION (1990), Paper No. 40.
11. Nordsveen, M., S. Nešić, R. Nyborg, and A. Stangeland, *Corrosion* 59 (2003): pp. 443–456.
12. Nešić, S., M. Nordsveen, R. Nyborg, and A. Stangeland, "A Mechanistic Model for CO_2 Corrosion with Protective Iron Carbonate Films," in CORROSION (2001), Paper No. 040.
13. Pots, B.F.M., "Mechanistic Models for the Prediction of CO2 Corrosion Rates under Multi-Phase Flow Conditions," in CORROSION (1995), p. Paper No. 137.
14. Kahyarian, A., B. Brown, and S. Nesic, *Corrosion* 72 (2016): pp. 1539–1546.

15. Tran, T., B. Brown, and S. Nešic, *Corrosion* 70 (2014): pp. 223–229.
16. Zheng, Y., B. Brown, and S. Nešic, *Corrosion* 70 (2014): pp. 351–365.
17. Esmaeely, S.N., B. Brown, and S. Nesic, *Corrosion* 73 (2017): pp. 144–154.
18. Tran, T., B. Brown, and S. Nešić, "Corrosion of Mild Steel in an Aqueous CO_2 Environment – Basic Electrochemical Mechanisms Revisited," in CORROSION (2015), paper no. 671.
19. Bockris, J.O., and D. Drazic, *Electrochim. Acta* 7 (1962): pp. 293–313.
20. Hibert, F., Y. Miyoshi, G. Eichkorn, and W.J. Lorenz, *J. Electrochem. Soc.* 118 (1971): pp. 1919–1926.
21. Atkinson, A., and A. Marshall, *Corros. Sci.* 18 (1978): pp. 427–439.
22. El Miligy, A.A., D. Geana, and W.J. Lorenz, *Electrochim. Acta* 20 (1975): pp. 273–281.
23. Nešić, S., N. Thevenot, J.L. Crolet, and D. Drazic, "Electrochemical Properties of Iron Dissolution in the Presence of CO_2 - Basics Revisited," in CORROSION (1996), Paper No. 03.
24. Keddam, M., O.R. Mattos, and H. Takenout, *J. Electrochem. Soc.* 128 (1981): pp. 257–266.
25. Keddam, M., O.R. Mattos, and H. Takenout, *J. Electrochem. Soc.* 128 (1981): pp. 266–274.
26. Felloni, L., *Corros. Sci.* 8 (1968): pp. 133–148.
27. Bockris, J.O., D. Drazic, and A. R. Despic, *Electrochim. Acta* 4 (1961): pp. 325–361.
28. Drazic, D., *Mod. Asp. Electrochem.* 19 (1989): pp. 62–192.
29. Dražić, D.M., and C.S. Hao, "The Anodic Dissolution Process on Active Iron in Alkaline Solutions," Electrochimica Acta (1982).
30. Lorenz, W.J., G. Staikov, W. Schindler, and W. Wiesbeck, *J. Electrochem. Soc.* 149 (2002): pp. K47--K59.
31. Keddam, M., "Anodic Dissolution," in Corros. Mech. Theory Pract. Third Ed. (CRC Press, 2011), pp. 149–215, http://dx.doi.org/10.1201/b11020-4.
32. Heusler, K.E., *Encyclopedia of Electrochemistry of the Elements. Vol. 9* (New york: Marcel Dekker, 1982).
33. Nešić, S., J. Postlethwaite, and S. Olsen, *Corrosion* 52 (1996): pp. 280–294.
34. Ogundele, G.I., and W.E. White, *Corrosion* 42 (1986): pp. 71–78.
35. George, K.S., and S. Nešic, *Corrosion* (2007): pp. 178–186.
36. Song, F.M., *Electrochim. Acta* 55 (2010): pp. 689–700.
37. Song, F.M., D.W. Kirk, J.W. Graydon, and D.E. Cormack, *J. Electrochem. Soc.* 149 (2002): pp. B479–B486, http://jes.ecsdl.org/cgi/doi/10.1149/1.1509068.
38. Anderko, A., and R.D. Young, "Simulation of CO2/H2S Corrosion Using Thermodynamic and Electrochemical Models," in Corros. 1999 (1999), p. Paper No. 31.
39. Han, J., J.W. Carey, and J. Zhang, *Int. J. Greenh. Gas Control* 5 (2011): pp. 777–787, http://dx.doi.org/10.1016/j.ijggc.2011.02.005.
40. Linter, B.R., and G.T. Burstein, *Corros. Sci.* 41 (1999): pp. 117–139.
41. Simard, S., M. Drogowska, H. Menard, and L. Brossard, *J. Appl. Electrochem.* 27 (1997): pp. 317–324, http://www.springerlink.com/index/K8085843X9737H61.pdf.
42. Castro, E.B., and J.R. Vilche, *Corros. Sci.* 32 (1991): pp. 37–50.
43. Davies, D.H., and T. Burstein, *Corrosion* 36 (1980): pp. 416–422.
44. das Chagas Almeida, T., M.C.E. Bandeira, R.M. Moreira, and O.R. Mattos, *Corros. Sci.* 120 (2017): pp. 239–250, http://dx.doi.org/10.1016/j.corsci.2017.02.016.
45. Farelas, F., M. Galicia, B. Brown, S. Nesic, and H. Castaneda, *Corros. Sci.* 52 (2010): pp. 509–517.
46. Yang, Y., "Removal Mechanisms of Protective Iron Carbonate Layer in Flowing Solutions," Ohio University, 2012, https://etd.ohiolink.edu/ap/10?0::NO:10:P10_ETD_SUBID:62105%5Cnfiles/55/10.html.
47. Li, W., "Mechanical Effects of Flow on CO_2 Corrosion Inhibition of Carbon Steel Pipelines," Ohio University, 2016.
48. Yang, Y., B. Brown, S. Nesic, M.E. Gennaro, and B. Molinas, "Mechanical Strength And Removal Of A Protective Iron Carbonate Layer Formed On Mild Steel In CO2 Corrosion," in CORROSION

(2010), p. paper no. 10383.
49. Li, W., B.F.M. Pots, B. Brown, K.E. Kee, and S. Nesic, *Corros. Sci.* 110 (2016): pp. 35–45, http://dx.doi.org/10.1016/j.corsci.2016.04.008.
50. Berger, F.P., and K.-F.F.-L. Hau, “Mass Transfer in Turbulent Pipe Flow Measured by the Electrochemical Method,” International Journal of Heat and Mass Transfer (1977).
51. Nešić, S., J. Postlethwaite, and N. Thevenot, *J. Corros. Sci. Eng.* 1 (1995): pp. 1–14.
52. Soli, A.L., and R.H. Byrne, *Mar. Chem.* 78 (2002): pp. 65–73.
53. Lorbeer, P., and W.J. Lorenz, *Corrosion* 20 (1980): pp. 405–412.
54. Lorenz, W.J., G. Staikov, W. Schindler, and W. Wiesbeck, *J. Electrochem. Soc.* 149 (2002): pp. K47--K59.
55. Tanupabrungsun, T., D. Young, B. Brown, and S. Nešić, *CORROSION* (2012): p. 1418.